REVISED

Simulating the fine and coarse inorganic particulate matter concentrations in a polluted Megacity

Vlassis A. Karydis[1], Alexandra P. Tsimpidi[1], Christos Fountoukis[1], Athanasios Nenes[1,2,3], Miguel Zavala[4], Wenfang Lei[4], Luisa T. Molina[4], Spyros N. Pandis[1,5,6]

[1]Institute of Chemical Engineering and High Temperature Chemical Processes (ICE-HT), Foundation for Research and Technology Hellas (FORTH), Patras, Greece

[2]School of Chemical and Biomolecular Engineering, Georgia Institute of Technology, Atlanta, GA

[3]School of Earth and Atmospheric Sciences, Georgia Institute of Technology, Atlanta, GA

[4]Department of Earth, Atmospheric and Planetary Sciences, Massachusetts Institute of Technology (MIT) and Molina Center for Energy and the Environment (MCE2), USA

[5]Department of Chemical Engineering, University of Patras, Patras, Greece

[6]Department of Chemical Engineering, and Department of Engineering and Public Policy, Carnegie Mellon University, Pittsburgh, PA 15213, USA

Abstract

A three dimensional chemical transport model (PMCAMx) is applied to the Mexico City Metropolitan Area (MCMA) in order to simulate the chemical composition and mass of the major PM_1 (fine) and PM_{1-10} (coarse) inorganic components and determine the effect of mineral dust on their formation. The aerosol thermodynamic model ISORROPIA-II is used to explicitly simulate the effect of Ca, Mg, and K from dust on semi-volatile partitioning and water uptake. The hybrid approach is applied to simulate the inorganic components, assuming that the smallest particles are in thermodynamic equilibrium, while describing the mass transfer to and from the larger ones. The official MCMA 2004 emissions inventory with improved dust and NaCl emissions is used. The comparison between the model predictions and measurements during a week of April of 2003 at Centro Nacional de Investigacion y Capacitacion Ambiental (CENICA) "Supersite" shows that the model reproduces reasonably well the fine mode composition and its

diurnal variation. Sulfate predicted levels are relatively uniform in the area (approximately 3 μg m^{-3}), while ammonium nitrate peaks in Mexico City (approximately 7 μg m^{-3}) and its concentration rapidly decreases due to dilution and evaporation away from the urban area. In areas of high dust concentrations, the associated alkalinity is predicted to increase the concentration of nitrate, chloride and ammonium in the coarse mode by up to 2 μg m^{-3} (a factor of 10), 0.4 μg m^{-3}, and 0.6 μg m^{-3} (75%), respectively. The predicted ammonium nitrate levels inside Mexico City for this period are sensitive to the physical state (solid versus liquid) of the particles during periods with RH less than 50%.

1. Introduction

Atmospheric suspended particles, or aerosols, range from a few nanometers to tens of micrometers in diameter and exert a significant impact on atmospheric processes. They influence visibility (Altshüller, 1984) and the planetary radiative balance by scattering and absorbing light. Aerosols also act as cloud condensation nuclei, and indirectly affect climate through changes in cloud reflectivity and lifetime through changes in droplet number concentration. Exposure to high concentrations of airborne particulate matter (PM) often results in serious human health problems (Schwartz, 1996; Borja-Aburto et al., 1998; Pope et al., 2002). Atmospheric aerosols are composed of water, inorganic salts, crustal material, organics, and trace elements. A large part of the particle mass (25-75%) is inorganic, with sulfates, nitrates, ammonium, sodium and chloride being the dominant species. Nitrate can be found in both fine (particles with diameters less than 1 μm) and coarse (particles with diameters larger than 1 μm) modes. Sodium, chloride and the crustal components are mainly found in the coarse mode while ammonium and sulfate are usually in the fine mode (Seinfeld and Pandis, 2006).

A portion of inorganic PM is generally classified as “crustal material” or “dust” with Ca, K, Mg, and Na being its major chemically-active constituents (e.g., Kim and Seinfeld, 1995; Jacobson, 1999b; Chow et al., 1993; Chan et al., 1997; Gillies et al., 2001; Vega et al., 2001; Marcazzan et al., 2001; Villasenor et al., 2002; Wang et al., 2007; Li et al., 2008; Adamo et al. 2007). Mineral dust tends to originate from specific areas in the Earth (Prospero et al., 2002) and then is transported over very long distances, influencing climate and atmospheric chemistry on regional and global scales (McKendry et al., 2001; Perry et al., 1997; Tratt et al., 2001). Climatic effects of mineral dust include reflection and absorption of incoming solar radiation (Buseck et

al., 2000) as well as impacts on cloud formation, cloud properties, precipitation (Feingold et al., 1999; Kumar et al., 2009; Mahowald and Kiehl, 2003; Rudich et al., 2002; Wurzler et al., 2000; Sun et al., 2008). Atmospheric chemistry of mineral dust modifies both the gas-to-particle partitioning in the atmosphere and physicochemical properties of individual particles (Dentener et al., 1996; Jacob, 2000; Bian and Zender, 2003; Laskin et al., 2005; Fountoukis et al., 2009). However, most global models oversimplify the chemistry of dust as the crustal materials are often considered as a single inert component (Bauer et al., 2004; Bian and Zender, 2003; Liao et al., 2003; Martin et al., 2003). In addition, only a few regional models simulate the heterogeneous chemistry of dust (Hodzic et al., 2006; Zaveri et al., 2008).

Three main approaches have been used to simulate aerosol-gas phase partitioning of semi-volatile species. In the "bulk equilibrium" approach (Pilinis et al., 1987; Russell et al., 1988; Binkowski and Shankar, 1995; Lurmann et al., 1997), the gas and aerosol phases are assumed to be always in equilibrium. This method neglects both the time required for mass transfer and the variation of composition with particle size. The advantage of this approach is its speed, simplicity, and stability. The "size-resolved equilibrium" approach allows in general a more accurate representation of the partitioning of semi-volatile species (Pilinis and Seinfeld, 1987; Pilinis et al., 1987; Jacobson et al., 1996; Lu et al., 1997; Kleeman et al., 1997). In this method the chemical composition of discrete and internally homogenous aerosol size sections generates size-specific driving forces for the partitioning of semivolatile components. However, mass transfer is still considered instantaneous. The major disadvantage of this approach is that infinite solutions to the problem may exist if the particles are solid (Wexler and Seinfeld, 1990). In the "dynamic" approach, active mass transfer is considered for each aerosol size "section" or "mode" (Meng and Seinfeld, 1996; Meng et al., 1998; Jacobson et al., 1996; Jacobson, 1997a, b; Sun and Wexler, 1998a, b; Pilinis et al., 2000; Zhang and Wexler, 2008; Zaveri et al., 2008). Although this approach is the most accurate, it is much more computationally intensive than the bulk equilibrium approach. By analyzing the equilibrium time scales for ammonium nitrate, Meng and Seinfeld (1996), Dassios and Pandis (1999) and Cruz et al. (2000) found that aerosol nitrate associated with the submicrometer size range equilibrates with the gas phase within a few minutes (i.e., less than the typical timestep of a chemical transport model). For particles much larger than approximately 1 μm, the assumption of thermodynamic equilibrium introduces substantial error, since their equilibrium timescale can be an hour or longer.

All aerosol simulations, either based on thermodynamic, dynamic, or hybrid approaches, require computation of equilibrium composition to drive the mass transfer. Several models have been developed for this purpose and differ in the chemical species that they can treat, the solution method used and the type of input they can accept. AIM2 (Clegg and Pitzer, 1992; Clegg et al., 1992, 1994, 1995, 1998a, b; Wexler and Clegg, 2002) and GFEMN (Ansari and Pandis, 1999a, b) use direct Gibbs free energy minimization methods to solve equilibrium problems for ammonium-nitrate-sulfate-sodium-chloride systems. UHAERO (Amundson et al., 2006) also minimizes the Gibbs free energy of the system offering a choice of the Pitzer, Simonson, Clegg (PSC) mole fraction-based model (Pitzer and Simonson, 1986; Clegg and Pitzer, 1992; Clegg et al., 1992) or the ExUNIQUAC model (Thomsen and Rasmussen, 1999) for the activity coefficient calculations. These models treat either the ammonium-nitrate-sulfate system or the ammonium-sodium-nitrate-chloride-sulfate system. MESA (Zaveri et al., 2005a; b) simultaneously iterates for all solid-liquid equilibria using a pseudo-transient continuation method and simulates the ammonium-sodium-nitrate-sulfate-chloride-calcium system of species. EQUISOLV II (Jacobson et al., 1996; Jacobson et al., 1999a, b) sequentially finds the root of each equation in the corresponding system of equilibrium equations and then iterates over the entire domain until convergence. SCAPE2 (Kim et al., 1993a, b; Kim and Seinfeld, 1995; Meng et al., 1995) divides the composition space into several subdomains based on major species that impact equilibrium partitioning and water uptake. Similar to SCAPE2, ISORROPIA (Nenes et al., 1998; Nenes et al., 1999) determines the subsystem set of equilibrium equations and solves for the equilibrium state using the chemical potential method. The code solves analytically as many equations as possible through successive substitutions; remaining equilibrium reactions are solved numerically using bisection to ensure stability. ISORROPIA also offers the choice of using precalculated tables of binary activity coefficients and water activities of pure salt solutions, which speeds up calculations by approximately 30%. Due to its computational efficiency, ISORROPIA is used in several three dimensional chemical transport models (CTM) including CMAQ (Binkowski and Roselle, 2003; Mebust et al., 2003; Yu et al., 2005) and PMCAMx (Gaydos et al., 2007; Karydis et al. 2007), and general circulation models (Adams and Seinfeld, 2002).

An important limitation of most thermodynamic models is the lack of treatment of crustal species (Ca, K, and Mg). Crustal material affects the partitioning of nitrate and ammonium,

especially in areas where dust comprises a significant portion of total PM, and the simulation of these effects can considerably improve model predictions (Jacobson, 1999b; Moya et al., 2002). An attempt to treat crustal species as "equivalent sodium" was met with modest success (Moya et al., 2001a). Moya et al. (2002) showed that including crustal species explicitly is important in determining the aerosol size distribution, while San Martini et al. (2005) showed that treating crustal species as "equivalent" sodium may affect the predicted response of inorganic PM to changes in precursor concentrations.

In the current study, we incorporate the new thermodynamic model ISORROPIA-II (Fountoukis and Nenes, 2007), in which the thermodynamics of the crustal elements of calcium, potassium and magnesium have been added to the preexisting suite of components of the ISORROPIA model, in a three dimensional CTM, PMCAMx (Gaydos et al., 2007). The new model combines the computational advantages of ISORROPIA with the explicit treatment of thermodynamics of crustal species. Size-resolved composition of particles is simulated using the hybrid method of Capaldo et al. (2000). This new inorganic modeling framework is applied in the Mexico City Metropolitan Area (MCMA) and is evaluated against measurements taken during the MCMA campaign in April of 2003 (Molina et al, 2007). Moreover, the effects of mineral dust and hybrid approach for the aerosol dynamics to the composition and the size distribution of the predicted inorganic aerosols are discussed.

2. PMCAMx Description

PMCAMx uses the framework of the CAMx air quality model (ENVIRON, 2003), which considers the processes of horizontal and vertical advection and dispersion, wet and dry deposition, and gas-phase chemistry. Three detailed aerosol modules have been implemented: inorganic aerosol formation (Gaydos et al., 2003; Koo et al., 2003), aqueous-phase chemistry (Fahey and Pandis, 2001), and secondary organic aerosol formation and growth (Lane et al., 2008). The aerosol species treated are sulfate, nitrate, ammonium, chloride, potassium, calcium, magnesium, elemental carbon, and primary and secondary organics. The aerosol size and composition distribution is simulated using a sectional representation across 10 size bins with the wet diameter varying from 40 nm to 40 μm. The chemical mechanism used is based on the SAPRC99 mechanism (Carter, 2000; Environ, 2003) which contains 211 reactions with 56 gases and 18 radicals. The overall performance of the SAPRC99 mechanism in simulating the amount

of O_3 formed and NO oxidized was satisfactory. In addition, reactivities of most VOCs were reasonably well simulated. , though in many cases adjustments to uncertain portions were made to achieve the fits (Lei et al., 2007).

2.1 Inorganic Aerosol Thermodynamics

New inorganic species were added in PMCAMx and linked with the inorganic modules in order to treat explicitly calcium, potassium, and magnesium cations which are considered as active components of mineral dust. Inorganic equilibrium composition was computed with the ISORROPIA-II model (Fountoukis and Nenes, 2007) which, compared to its predecessor ISORROPIA (Nenes et al., 1998) has been extended to include crustal elements using 10 additional salts ($Ca(NO_3)_2$, $CaCl_2$, $CaSO_4$, $KHSO_4$, K_2SO_4, KNO_3 , KCl, $MgSO_4$, $Mg(NO_3)_2$, $MgCl_2$) in the solid phase and 3 more ions (Ca^{2+}, K^+, Mg^{2+}) in the aqueous phase. Additional improvements in ISORROPIA-II include updated water activity database, temperature dependency of the activity coefficients, mutual deliquescence relative humidity points, activity coefficient calculation algorithm and tabulated Kusik-Meissner binary activity coefficient data. Details about ISORROPIA-II can be found in Fountoukis and Nenes (2007).

2.2 Inorganic Aerosol Growth

Simulation of the effects of mineral dust on inorganic semivolatile species partitioning requires an accurate description of the aerosol dynamics in the coarse mode while it is desirable for the model to be computational efficient for future routine applications. In this work we use the hybrid method for aerosol dynamics developed by Capaldo et al. (2000) in which the aerosol particles with diameters less than the threshold diameter (1 μm for the purposes of this study) are simulated assuming equilibrium. The bulk equilibrium approach used in this work assumes instantaneous mass transfer with PM, the composition determined by applying ISORROPIA-II. At a given time step the sum of the gas and fine aerosol fraction are provided to ISORROPIA-II, which evaluates the partitioning between the two phases assuming that the aerosols can form solids (“stable” solution). The sensitivity of our results to this assumption is discussed in a subsequent section. The material transferred between phases is distributed over the aerosol size distribution by using weighting factors for each aerosol size section (Pandis et al., 1993). For particles larger than the threshold diameter the improved MADM model of Pilinis et al. (2000),

as extended by Gaydos et al. (2003), is used, which ensures a stable solution, regardless if the particles are completely dry, with an aqueous phase or transition between acidic and neutral conditions. The calculations of fine and coarse mode composition are decoupled and computed sequentially. First, the gas phase is allowed to equilibrate with the fine aerosol mode. MADM then integrates the mass transfer differential equations for the coarse mode sections using the gas-phase concentrations calculated by the equilibrium step.

3. Model Application

PMCAMx is used to simulate air quality in the Mexico City Metropolitan Area (MCMA) during 12-16 April of 2003, which was a pollution episode characterized by stagnant meteorological conditions and high pollutant concentration in the south of the city (de Foy et al., 2005). Also in part due to the availability of gas and aerosol ambient measurements, this period has been a focus of extensive gas-phase photochemical modelling studies to evaluate aerosol precursor emissions and ozone formation (Lei et al., 2007, 2009). The first day of each simulation has been excluded in order to limit the effect the initial conditions have on the results. One day is sufficient for such relatively small urban modelling domains. The values of the organics, elemental carbon, nitrate, sulfate, ammonium and mineral dust concentrations at the boundaries of the domain were chosen based on results of the GISS-II' global CTM (Racherla et al., 2006) which uses present-day emissions and prescribed sea-surface temperatures. These results generate a climatological background of aerosols in the area around the PMCAMx model domain with the aerosol values representing a 5-year average for the month of April. The values of the major inorganic aerosol concentrations at the boundaries of the domain are shown in Table 1. Sulfate concentrations are high in the north and west side of the domain while sodium chloride is high in the south side. The PMCAMx modelling domain covers a 156x156x6 km region centered in the MCMA with 3x3 km grid resolution and fifteen vertical layers extending to 6 km. Meteorological inputs to the model include horizontal wind components, temperature, pressure, water vapor, vertical diffusivity, clouds, and rainfall, all computed offline by the MM5 meteorological model (Grell et al., 1995). The MM5 simulation and evaluation are described in detail by de Foy et al. (2006a, b). These authors concluded that the main features of the Mexico basin flow are well represented by the model for the simulation period.

The emission inventory used is constructed from the MCMA 2004 official emission inventory (SMA-DF, 2006) with improved dust and sodium chloride emissions. An extensive array of data from the air quality monitoring network and intensive campaign observations were used to constrain the emissions of ozone precursors, including CO, NOx and speciated volatile organic compounds (VOC) (Lei et al., 2007; 2009). The emission rates of SO_2, NH_3, and NO_x, which represent the gas precursors of the major inorganic components, are the same for each of the simulation days and are equal to 17.7, 54.4 and 350.9 tons d^{-1} respectively. The estimated emission rates from resuspension of particles, both from wind erosion (non road) and from traveling vehicles (on road), are 0.4 tons d^{-1} primary sulfate, 0.2 tons nitrate and 0.3 tons ammonium. The emission rate of sodium chloride is 2.5 tons d^{-1}. Dust emissions were estimated following the EPA bottom-up approach using wind erosion emission factors by land use type and vegetation coverage mounted on a Geographical Information System. The improved dust emissions are the only emissions which are different for each day of simulation and they were calculated based on the algorithm of Draxler et al. (2001). In brief, the emissions of wind-blown dust are a function of threshold friction velocity (which is dependent of surface roughness), friction velocity and the surface soil texture. The friction velocity and threshold friction velocity were calculated from the same MM5 meteorology that was used to drive PMCAMx. The geographical distribution and strength of the dust emissions are determined by the landuse, soil texture and simulated meteorology. The PM_{10} dust emission rates fluctuated from 1,400 tons d^{-1} to 170 tons d^{-1} depending on wind speed with an average value equal to 800 tons d^{-1}. Approximately 70% of these emissions are distributed in particles with diameter 2.5-10 μm. Calcium, potassium, and magnesium emissions, which are the reactive dust components, represent 2.4%, 1.5%, and 0.9% of the total dust emissions respectively based on the global average abundance of these elements in soil and crustal rock (Sposito, 1989).

4. Predicted Inorganic Aerosol Concentrations

The average predicted PM_1 (fine) ground level concentrations of sulfate, nitrate, ammonium, chloride, and sodium during April 13-16 are depicted in Figure 1. Selected sites in Mexico City appear in this figure and their description is listed in Table 2. Sulfate concentrations are relatively homogeneous across the city varying from 1.5 μg m^{-3} in the southeast to 2.5 μg m^{-3} inside Mexico City. The average diurnal concentration profile of the predicted sulfate in the

center of Mexico City shows little variation (mean value equal to 2.5 μg m^{-3} and standard deviation equal to 0.5 μg m^{-3}) indicating that most of it is from regional transport, a result consistent with field measurements from different campaigns. In the late 1990, as a part of the Aerosol and Visibility Evaluation Research (IMADA-AVER) campaign, Chow et al. (2002a) measured sulfate concentrations at the city boundaries that were about two-thirds of the concentrations measured within the urban area. Salcedo et al. (2006) has presented evidence that gas-phase sulfate production in the MCMA is a minor contributor to the observed concentrations. DeCarlo et al. (2008) also observed the low variability of the sulfate levels in the area using aircraft data collected over Mexico City and Central Mexico during MILAGRO.

Predicted PM_1 nitrate is found to be higher in city center (up to 4.5 μg m^{-3}), mostly produced from local photochemistry, and decreases with distance from the city, due to evaporation and deposition, remaining at low levels in the surrounding area (lower than 1 μg m^{-3}). These predictions are in agreement with the measured nitrate decreases with distance from the city during the MILAGRO campaign (DeCarlo et al., 2008). Ammonium concentrations also peak at the center of Mexico City (up to 2 μg m^{-3}) and follow the same spatial distribution with that of nitrate because these two species exist in the model mainly in the form of NH_4NO_3, consistent with observations during MCMA-2003 (Salcedo et al., 2006: San Martini et al., 2006) and MILAGRO (Zheng et al., 2008; Hennigan et al., 2009; Aiken et al., 2009). However, ammonium interacts with the regional sulfate forming $(NH_4)_2SO_4$ with ammonium concentrations up to 1 μg m^{-3}. PM_1 Chloride and sodium have similar spatial distributions with high concentrations in the south of the domain (around 0.5 μg m^{-3} and 0.8 μg m^{-3}, respectively), contrary to ammonium nitrate which is predicted to be high in the center of Mexico City.

The average predicted coarse, PM_{1-10}, ground level concentrations of the chemically unreactive (inert) dust, calcium, potassium, magnesium, nitrate, ammonium, and chloride during April 13-16 are depicted in Figure 2. The model predicts high levels of PM_{1-10} dust in most of the model domain during this period which in some areas are higher than 25 μg m^{-3}. The highest concentration (40 μg m^{-3}) is predicted in the vicinity of Lake Texcoco, which is the major source of dust in Mexico City (Chow et al., 2002b; Moffet et al., 2008). The layers near the surface of this lake consist of volcanic glass and feldespathic pyroclasts in the sand fraction (250-500 μm), feldspar, cristobalite, calcite, and dolomite in the silt fraction (2-50 μm) and cristobalite, plagioclase and smectite in clay fraction (<2 μm) (Gutierrez-Castorena et al., 2005). The

microprobe analysis of the groundmass of the lake points to a dominance of SiO_2 with smaller amounts of Al_2O_3, FeO_3, CaO, K_2O, and MgO. Calcium, potassium, and magnesium are a small fraction of the coarse PM and their concentrations are predicted to be relatively low (up to 0.7 μg m^{-3}, 0.5 μg m^{-3}, and 0.3 μg m^{-3} respectively) with spatial distribution similar to that of the inert dust (Figure 2). Nevertheless, the presence of these components affects the mass transfer of nitric and hydrochoric acid to/from the coarse particles. Coarse nitrate is predicted to be up to 2 μg m^{-3} at Lake Texcoco and the surrounding areas, while coarse chloride over the same areas is predicted to be up to 1.2 μg m^{-3}. Coarse chloride levels are slightly higher in the south of the domain.

5. Model Evaluation

5.1 Inorganic fine PM

The model predictions for fine sulfate, nitrate, ammonium, chloride and crustal material were compared with measurements that took place during the Mexico City Metropolitan Area field campaign at a highly instrumented "Supersite" located at the "Centro Nacional de Investigacion y Capacitacion Ambiental" (CENICA), in southeast Mexico City (Salcedo et al., 2006). CENICA is located in a mixed commercial-residential area with relatively few industries or congested road networks, and was thus assumed to be representative of average urban conditions. During the MCMA-2003 campaign, an Aerodyne Quadrupole Aerosol Mass Spectrometer (Q-AMS) was deployed at CENICA, measuring the size-resolved aerosol chemical composition of non-refractory species in particles smaller than about 1 μm with a 4 minute time resolution (Jayne et al., 2000; Jimenez et al., 2003). An AMS collection efficiency (CE) of 0.5 was used based on multiple intercomparisons with other aerosol measurements (Salcedo et al., 2006; Johnson et al., 2008; Dzepina et al., 2009), as well as other AMS studies in Mexico City (Kleinman et al., 2008; DeCarlo et al., 2008; Aiken et al., 2009). The results of the comparison between the model predictions and the measurements are depicted in Figure 3. The mean bias (MB), mean absolute gross error (MAGE), normalized mean bias (NMB), normalized mean error (NME), and the root mean square error (RMSE) were also calculated (Table 3) to assess the model performance:

$$MAGE = \frac{1}{N}\sum_{i=1}^{N}\left|P_i - O_i\right| \qquad MB = \frac{1}{N}\sum_{i=1}^{N}(P_i - O_i)$$

$$NME = \frac{\sum_{i=1}^{N} |P_i - O_i|}{\sum_{i=1}^{N} O_i} \qquad NMB = \frac{\sum_{i=1}^{N} (P_i - O_i)}{\sum_{i=1}^{N} O_i}$$

$$RMSE = \left[\frac{1}{N} \sum_{i=1}^{N} (P_i - O_i)^2 \right]^{\frac{1}{2}}$$

where P_i is the predicted value of the pollutant concentration, O_i is the observed value of the pollutant at the same time, and N is the total number of the predictions used for the comparison. NME (in %) and MAGE (in μg m^{-3}) give an estimation of the overall discrepancy between predictions and observations, while NMB (in %) and MB (in μg m^{-3}) are sensitive to systematic errors. RMSE (in μg m^{-3}) is the root of the mean square error which incorporates both the variance of the prediction and its bias. Additional details for the above evaluation metrics can be found in Yu et al. (2006). The predicted and the measured values are compared for every single hour during the simulation period, instead of the usual comparison of daily average PM values (Morris et al., 2006), resulting in relatively higher MAGE and NME values (Table 2).

Sulfate: The model performs reasonably well in CENICA for most of the simulation period (Figure 3). The average predicted concentration of sulfate is 2.4±0.5 μg m^{-3} while the average measured value is 2.9±1 μg m^{-3}. The major sources of sulfur dioxide near MCMA are the Tula refineries which are located approximately 100 km north-northwest of Mexico City center and are not included in our model domain. Therefore, when the meteorology favors the transport of the Tula emissions to Mexico City, high concentrations of sulfate can be observed in the urban center. That is the case during the fourth day (April 15th) of our simulation period. The model though, is unable to capture those episodes as the boundary conditions are assumed to be constant. The NME and the NMB excluding the data point at seven o'clock in the evening of the third day are 27% and -16% respectively which indicates an encouraging performance.

Nitrate: Both PMCAMx and measurements suggest that PM_1 nitrate is approximately 3 μg m^{-3} on average and peaks during noon with concentrations up to 16 μg m^{-3}. The performance of the model is satisfactory during the fourth (April 15th), and the fifth (April 16th) simulation day as the predicted and the measured timeseries at CENICA are in agreement (MAGE=1.7 μg

m^{-3}). The model though tends to underestimate nitrate during these days with a MB equal to -1.7 μg m^{-3}. On the other hand, during the first and the second day, the model is slightly overpredicting nitrate (ME=1.4 μg m^{-3}). This overprediction may be related to the ammonia emissions and its day-to-day variations. The model predicts significant PM_1 nitrate concentrations (above 5 μg m^{-3}) also during the first and the second afternoon. Both predicted peaks are in periods when the RH was less than 50% and therefore their magnitude will be sensitive to the physical state of the aerosol (wet versus dry) (Ansari and Pandis, 2000). During nighttime, predicted nitrate remains low (a few μg m^{-3}), which is consistent with the measurements.

Ammonium: Predictions and measurements are in reasonable agreement during the fourth (April 15th) and the fifth (April 16th) day (MAGE=0.9 μg m^{-3}), while there is a slight overprediction during the second (April 13th) and the third (April 14th) day (NMB=7%). This indicates that the variation of ammonium is determined by nitrate, as sulfate is a regional component with little daily variation. Nevertheless, there is a period of high ammonium (~3.5 μg m^{-3}) in the measurements, during the fourth (April 15th) evening, which is related to the sulfate coming from the Tula refineries and which the model is unable to capture. Similar to nitrate, PM_1 ammonium peaks every noon with concentrations up to 5 μg m^{-3}, while a significant PM_1 ammonium concentration peak (above 2 μg m^{-3}) is also predicted during the first and the second afternoon. Some ammonium exists in the aerosol phase even at night, mainly in the form of ammonium sulfate, with concentrations approximately 1 μg m^{-3}. On average, PMCAMx predicts 1.4±1.3 μg m^{-3} of PM_1 ammonium, which is well within the observed range (1.8±0.9 μg m^{-3}).

Chloride: In the MCMA, fine chloride concentrations in the urban center peak during morning, but rarely exceed 0.5 μg m^{-3}. The model overall reproduces observations, but did not simulate three concentration "spikes" observed during the second (April 13th) (0.9 μg m^{-3}), the fourth (April 15th) (0.6 μg m^{-3}), and the fifth (April 16th) (1.6 μg m^{-3}) morning. As a result, PMCAMx underpredicts the average concentration of PM_1 chloride by roughly a factor of two (predicted: 0.1±0.1 μg m^{-3}; observed: 0.2±0.2 μg m^{-3}). The MAGE and the MB excluding the data points from those three episodes are 0.09 and -0.01 μg m^{-3} respectively. Considering that the AMS measures chloride only in the form of NH_4Cl, the model underprediction of the ambient chloride concentrations is probably greater. Johnson et al. (2006) reported that 0.07 μg m^{-3} of chloride on average in CENICA during 13th-16th of April came from biomass burning.

Crustal Material: Johnson et al. (2006; 2008) used Proton-Induced X-ray Emission (PIXE) to determine the aerosol composition in the MCMA at CENICA during April of 2003. The $PM_{2.5}$ dust/soil particle concentration was estimated to be 2.2 μg m^{-3} on average for the month of April 2003 while PMCAMx predicted 2 μg m^{-3} on average for the period of 13^{th}-16^{th} of April 2003. The predicted $PM_{2.5}$ magnesium concentration is 30 ng m^{-3} that is consistent with the concentration derived from the PIXE analysis (approximately 25 ng m^{-3}) during the same period (13^{th}-16^{th} of April). Potassium is predicted to be 55 ng m^{-3} while the average value from the PIXE analysis during 13^{th}-16^{th} of April is 190 ng m^{-3}. This discrepancy is due to the lack of biomass burning emissions in the emission inventory used in this study which is the major source of potassium in Mexico City (Johnson et al., 2006). The measured calcium at CENICA (170 ng m^{-3}) for the period of 13^{th}-16^{th} of April is two times higher than the predicted value (85 ng m^{-3}) during the same period. Part of it may be due to the cement plant at Tula which is outside of the modeling domain.

5.2 Inorganic coarse PM

Due to the lack of suitable PM coarse composition measurements during the 2003 episode, the model predictions for coarse particles can be only compared with measurements that took place during the IMADA-AVER 1997 and the MILAGRO 2006 campaigns. In the coarse mode, dust represents on average 70% of the PM_{10} mass throughout the model domain. During the 1997 IMADA-AVER campaign, crustal material was the largest component of $PM_{2.5-10}$ constituting approximately 85% of the measured $PM_{2.5-10}$ mass (Chow et al., 2002b). The predicted mineral dust has similar spatial distribution with the corresponding footprint in the field analysis of Moffet et al. (2008) during the MILAGRO campaign. PMCAMx however cannot represent the observed high concentrations of dust northwest of Mexico City, as they originate from sources outside the model domain (cement plants near Tula). The predicted high concentrations of dust (30-40 μg m^{-3}) in the area downwind (north) of the Texcoco Lake are consistent with the measured values (43 μg m^{-3} on average) during the IMADA-AVER campaign (Chow et al., 2002b) in the Xalostoc site which is located 5 km west of the dry lake. The predicted coarse nitrate, ammonium, and sulfate are consistent with the measured values of ammonium sulfate and ammonium nitrate (approximately 1 μg m^{-3}) in MCMA during the IMADA-AVER campaign (Chow et al., 2002b).

6. Effects of Mineral Dust on the Semivolatile Inorganic Aerosol Formation

To estimate the effects of mineral dust on the formation of the semivolatile inorganic aerosol components, the predictions of the updated model were compared with those of the previous version (PMCAMx-2004 as described in Gaydos et al., 2007) which ignored the presence of the reactive dust components and used the equilibrium approach for the simulation of the partitioning of semivolatile inorganic PM components. The concentration difference in the coarse mode between the predictions of these two models for nitrate, chloride, and ammonium is shown in Figure 4. Positive concentrations reflect increases due to the treatment of dust chemistry.

In areas where the dust concentration levels are high, species such as nitrate and chloride, are associated with non-volatile mineral cations (Ca^{2+}, K^{+}, Mg^{2+}) forming salts in order to maintain the charge balance in the aerosol phase. This is not reflected in the PMCAMx-2004 simulations, where coarse mode nitrate is very low; the new modeling framework predicts up to 2 μg m^{-3} coarse mode nitrate. In such areas, the predicted coarse chloride is approximately 0.6 μg m^{-3} higher than the PMCAMx-2004 predictions.

Ammonium also increases in the coarse mode by using the new modeling framework. This change (up to 0.4 μg m^{-3}) at first seems counterintuitive, given that the coarse-mode particles are alkaline. The increase can be explained in terms of the reaction:

$$NH_3(g) + HNO_3(g) \leftrightarrow NH_4^+(aq) + NO_3^-(aq)$$

The addition of the soluble crustal elements, especially magnesium, increase the water content in the coarse mode which eventually shifts this reversible reaction to the aerosol phase producing more ammonium nitrate (Nguyen et al., 1997; Finlayson-Pitts and Pitts, 2000). Appreciable amounts of aerosol water (hence nitrate) is present even at moderate RH, given that some of the mineral salts deliquesce at low to moderate RH (e.g. 33% for $MgCl_2$ and 54% for $Mg(NO_3)_2$ at 298K).

In order to further investigate the individual influence of the hybrid approach and the thermodynamic model ISORROPIA-II on the results, one more simulation was conducted using ISORROPIA-II along with the bulk equilibrium approach for all size sections. The predictions of these three different modeling approaches are compared in Teotihuacan which is located

approximately 25 km north-northwest of the drained Lake Texcoco and thus the dust concentration levels are high (approximately 25 μg m^{-3}) (Figure 5). The predicted total PM nitrate using ISORROPIA-II along with the equilibrium approach is approximately 1 μg m^{-3} (71%) higher on average than applying ISORROPIA and assuming bulk equilibrium. This increase is due to the formation of salts ($Ca(NO_3)_2$, KNO_3, $Mg(NO_3)_2$) with the dust components considered by ISORROPIA-II. However, the bulk equilibrium algorithm distributes 91% of total PM nitrate to the fine mode that has most of the surface area. In the hybrid approach, the coarse fraction continues to absorb nitric acid vapors, even after the small particles achieve equilibrium, thus lowering the nitric acid gas-phase concentration. The smallest sections then lose mass as evaporation is required to maintain equilibrium with the gas phase. As a result the predicted coarse nitrate using ISORROPIA-II along with the hybrid approach represents 86% of the total PM nitrate.

The results using the new modeling framework for chloride and ammonium are similar to those of nitrate. PM_{10} chloride is 0.5 μg m^{-3} (71%) higher than the predicted chloride by PMCAMx-2004 while 89% of it is distributed in the coarse mode. PM_{10} ammonium is 0.2 μg m^{-3} (27%) higher on average than the predicted ammonium using PMCAMx-2004 and 40% of it exists in the coarse mode.

Overall, the use of the new thermodynamic model ISORROPIA-II results in an increase to the aerosol concentration of the semivolatile inorganic species while the hybrid approach is considered essential in order to simulate the influence of the dust components to the size distribution of the inorganic aerosols.

7. Sensitivity to the aerosol state assumption

A sensitivity test, where the aerosols are assumed to be metastable (i.e., always an aqueous solution down to very low RH), is used to investigate the impact of aerosol phase state on the simulations. Ansari and Pandis (2000) and Fountoukis et al. (2009) suggest that the stable state results in higher concentrations of PM ammonium nitrate than the metastable state when RH is lower than 50%. In the center of Mexico City, the RH is on average lower that 50% in these area, predicted PM_{10} ammonium nitrate assuming stable aerosol is higher (by 2 μg m^{-3}) than the metastable state case (Figure 6). Outside Mexico City, the RH is on average higher than

50%, aerosol is always an aqueous solution and stable and metastable aerosol simulations are in close agreement (Figure 6).

The metastable state assumption can also affect the size distribution of the aerosols in areas where crystallization is feasible. The predicted PM_{1-10} nitrate and PM_{1-10} ammonium, assuming "metastable" aerosols, are approximately 0.5 μg m^{-3} (35%) and 0.1 μg m^{-3} (25%) higher than the corresponding predictions assuming "stable" aerosols (Figure 6), even though the PM_{10} NH_4NO_3 is lower. This behavior is due to the repartitioning of nitrate from the fine (where its formation is not favorable any more) to the coarse mode.

The differences between stable and metastable solution predictions compared to measurements for PM_1 nitrate are depicted in Figure 7. The metastable branch predictions are in better agreement with the measurements during April 13^{th}-14^{th} compared to the stable solution results. From the night of April 15^{th}, and on, RH remained lower than 60%, reaching a minimum of 15%. This likely allowed the aerosol to crystallize, and remain solid throughout this dry period. As a result, PM_1 nitrate observations correlate better with the stable solution results during the last two simulation days. During the periods of low RH the dust concentration remained low and thus did not affect the crystallization processes. The possibility that the Mexico City aerosol is sometimes stable and sometimes metastable has been also reported by Fountoukis et al. (2009) and deserves further investigation.

8. Conclusions

The new thermodynamic model ISORROPIA-II was incorporated in a three dimensional chemical transport model, PMCAMx. ISORROPIA-II is based on the original ISORROPIA code, which was initially used by PMCAMx, and treats the thermodynamics of K^+-Ca^{2+}-Mg^{2+}-NH_4^+-Na^+-SO_4^{2-}-NO_3^--Cl^--H_2O aerosol systems. In addition, the hybrid approach was used to simulate the aerosol growth. This approach simulates the mass transfer to the fine aerosol sections (up to 1 μm) using the bulk equilibrium assumption and to the remaining aerosol sections using the dynamic approach and MADM. The model was applied in the MCMA for approximately a week during April of 2003. PMCAMx had reasonable performance for the major inorganic PM components. The absence of the Tula emissions though, which is a source of SO_2 during some periods in MCMA, resulted in discrepancies for a few hours during the simulated period between ammonium sulfate predictions and measurements at CENICA. The

nitrate predictions were satisfactory on average (mean bias of -0.1 μg m^{-3}), but the mean absolute gross error was 2.3 μg m^{-3} for the hourly PM_1 nitrate measurements that had peaks of around 15 μg m^{-3}. Moreover, PMCAMx overpredicted ammonium nitrate in some cases due to the use of the same ammonia emissions for each simulation day. The existence of the aerosol in a metastable state during part of the simulation can also explain some of the discrepancy.

The use of the ISORROPIA-II model assists in simulating the formation of PM nitrate and chloride as it includes interactions between these anions and the cations of mineral dust. In particular, PM_{10} nitrate and chloride at CENICA were 0.7 μg m^{-3} and 0.4 μg m^{-3} higher on average respectively than the predicted concentrations using the original code of ISORROPIA. In addition, the hybrid (or dynamic) approach is considered essential for predicting the influence of dust in the size distribution of the inorganic species as it simulates better the competition between small and large particles for condensable vapors in environments with significant dust concentrations. The new modeling framework predicts that 86% of the total PM nitrate and 89% of the total chloride at Teotihuacan is in the coarse mode instead of 9% and 59% respectively predicted by the model using the original code of ISORROPIA along with the equilibrium approach for all size sections. These fractions are lower as one moves away from the dust source regions. At CENICA the predicted decrease in PM_1 nitrate, which was induced by the increase in the coarse mode, improved the performance of the model compared with measurements. The NMB for PM_1 nitrate was 32% while the NMB by using the new modeling framework is -3%. The addition of the dust components causes an increase to the coarse ammonium too, due to thermodynamic interactions with the rest of the ions in the aqueous phase. The predicted coarse ammonium at Teotihuacan corresponds to 15% of the total PM ammonium.

The model predictions for nitrate inside Mexico City are sensitive to the aerosol state assumption at low RH (<50%). In particular, the stable state case predicted higher ammonium nitrate (up to 2 μg m^{-3}) compared to the metastable state case in the center of Mexico City. During two simulation days, the observations of the PM_1 nitrate at CENICA correlate with the meatstable state case predictions while during the last two days measurements are in a better agreement with the stable state case results.

Acknowledgments

We thank D. Salcedo, K. Dzepina and J. L. Jimenez for the AMS data from CENICA and J. L. Jimenez for his comments on the manuscript. This research was supported by the European Union and the 7th framework programme under the project MEGAPOLI (Grant agreement 212520). A. P. Tsimpidi, V. A. Karydis, and M. Zavala were partially supported by a scholarship from the Molina Center for Energy and the Environment. C. Fountoukis was partially suppported from a Marie Curie International Reintegration Grant. A. Nenes acknowledges NOAA (NMRAC000-5-04017). LTM acknowledges support from NSF (ATM-0528227).

References

Adamo P., Giordano S., Naimo D., and Bargagli R., 2008. Geochemical properties of airborne particulate matter (PM_{10}) collected by automatic device and biomonitors in a Mediterranean urban environment. Atmospheric Environment 42, 346-357.

Adams P.J., and Seinfeld J.H., 2002. Predicting global aerosol size distributions in general circulation models. J. Geophys. Res. 104, 13791-13823, doi:10.1029/2001JD001010.

Aiken, A.C., D. Salcedo, M.J. Cubison, et al. Mexico City Aerosol Analysis during MILAGRO using High Resolution Aerosol Mass Spectrometry at the Urban Supersite (T0). Part 1: Fine Particle Composition and Organic Source Apportionment. Atmospheric Chemistry and Physics Discussions, 9, 8377-8427, 2009.

Altshüller A.P., 1984. Atmospheric particle sulfur and sulfur dioxide relationships at urban and nonurban locations. Atmospheric Environment 18, 1421–1431.

Amundson N.R., Caboussat A., He J.W., Martynenko A.V., Savarin V.B., Seinfeld J.H., and Yoo K.Y., 2006. A new inorganic atmospheric aerosol phase equilibrium model (UHAERO), Atmospheric Chemistry and Physics 6, 975–992.

Ansari A.S. and Pandis S.N., 1999a. Prediction of multicomponent inorganic atmospheric aerosol behavior. Atmospheric Environment 33, 745–757.

Ansari A.S. and Pandis S.N., 1999b. An analysis of four models predicting the partitioning of semivolatile inorganic aerosol components. Aerosol Science and Technology 31, 129–153.

Ansari A.S. and Pandis S.N., 2000. The effect of metastable equilibrium states on the partitioning of nitrate between the gas and aerosol phases. Atmospheric Environment 34, 157–168.

Artaxo P., Oyola P., and Martinez R., 1999. Aerosol composition and source apportionment in Santiago de Chile. Nuclear Instruments & Methods in Physics Research Section B-Beam Interactions with Materials and Atoms 150, 409-416.

Bauer S.E., Balkanski Y., Schulz M., Hauglustaine D.A., and Dentener F., 2004. Global modeling of heterogeneous chemistry on mineral aerosol surfaces: Influence on tropospheric ozone chemistry and comparison to observations. Journal of Geophysical Research 109, D02304, doi:10.1029/2003JD003868.

Bian H.S. and Zender C.S.,2003. Mineral dust and global tropospheric chemistry: Relative roles of photolysis and heterogeneous uptake. Journal of Geophysical Research 108, 4672, doi:10.1029/2002JD003143.

Binkowski F.S. and Roselle S.J., 2003. Models-3 community multiscale air quality (CMAQ) model aerosol component - 1. Model description. Journal of Geophysical Research-Atmospheres 108, doi:10.1029/2001JD001409.

Binkowski F.S., Shankar U., 1995. The regional particulate matter model: 1. Model description and preliminary results. Journal of Geophysical Research-Atmospheres 100, 26191-26209.

Borja-Aburto V.H., Castillejos M., Gold, D.R., Bierzwinski S., and Loomis D., 1998. Mortality and ambient fine particles in Southwest Mexico City, 1993–1995. Environ. Health Perspectives 106, 849–855.

Bromley L.A., 1973. Thermodynamic properties of strong electrolytes in aqueous solutions. AICHE Journal 19, 313-320.

Buseck P.R., Jacob D.J., Posfai M., Li J., and Anderson J.R., 2000. Minerals in the air: An environmental perspective. International Geology Review 42, 577–593.

Capaldo K. P., Pilinis C. and Pandis S. N., 2000. A computationally efficient hybrid approach for dynamic gas/aerosol transfer in air quality models. Atmospheric Environment 34, 3617–3627.

Carter W.P.L.: Implementation of the SAPRC-99 chemical mechanism into the models-3 framework, http://pah.cert.ucr.edu/ftp/pub/carter/pubs/s99mod3.pdf, access: February 25, 2008.

Chan Y.C., Simpson, R.W., Mctainsh G.H., Vowles P.D., Cohen D.D., and Bailey G.M., 1997 Characterisation of chemical species in PM2.5 and PM10 aerosols in Brisbane, Australia. Atmospheric Environment 31, 3773-3785.

Chow J.C., Watson J.G., Lowenthal D.H., Solomon P.A., Magliano K.L., Ziman S.D., Richards L.W., 1993. PM_{10} and $PM_{2.5}$ compositions in California San Joaquin Valley. Aerosol Science and Technology 18, 105-128.

Chow J.C., Watson J.G., Edgerton S.A., Vega E., and Ortiz E., 2002a. Spatial differences in outdoor PM_{10} mass and aerosol composition in Mexico. Journal of The Air & Waste Management Association 52, 423-434.

Chow J.C., Watson J.G., Edgerton S.A., and Vega E., 2002b. Chemical composition of $PM_{2.5}$ and PM_{10} in Mexico City during winter 1997. Science Total Environment 287, 177–201.

Clegg S.L. and Pitzer K.S., 1992. Thermodynamics of multicomponent, miscible, ionic solutions: generalized equations for symmetrical electrolytes, Journal of Physical Chemistry 96, 3513–3520.

Clegg S.L., Pitzer K.S., and Brimblecombe P., 1992. Thermodynamics of multicomponent, miscible, ionic solutions. II. Mixture including unsymmetrical electrolytes. Journal of Physical Chemistry 96, 9470–9479.

Clegg S.L., Brimblecombe P., and Wexler A.S., 1998a. Thermodynamic model of the system H^+–NH^+_4 –SO^{2-}_4– NO^-_3–H_2O at tropospheric temperatures. Journal of Physical Chemistry 102, 2137–2154.

Clegg S.L., Brimblecombe P., and Wexler A.S., 1998b. Thermodynamic model of the system H^+–NH^+_4–Na^+–SO_4^{2-}–NO_3^-–Cl^-–H_2O at 298.15 K. Journal of Physical Chemistry 102, 2155–2171, 1998b.

Cruz C.N., Dassios K.G., and Pandis S.N., 2000. The effect of dioctyl phthalate films on the ammonium nitrate aerosol evaporation rate. Atmospheric Environment 34, 3897-3905.

Dassios K.G., Pandis S.N., 1999. The mass accommodation coefficient of ammonium nitrate aerosol, Atmospheric Environment 33, 2999-3003.

DeCarlo, P.F. et al., 2008. Fast airborne aerosol size and chemistry measurements above Mexico City and Central Mexico during the MILAGRO campaign. Atmospheric Chemistry Physics 8, 4027-4048.

de Foy, B., Caetano, E., Magana, V., Zitacuaro, A., Cardenas, B., Retama, A., Ramos, R., Molina, L. T., and Molina, M. J., 2005. Mexico City basin wind circulation during the MCMA-2003 field campaign, Atmos. Chem. Phys., 5, 2267–2288.

de Foy, B., Clappier, A., Molina, L. T., and Molina, M. J., 2006a. Distinct wind convergence patterns due to thermal and momentum forcing of the low level jet into the Mexico City basin, Atmos. Chem. Phys., 6, 1249–1265.

de Foy, B., Molina, L. T., and Molina, M. J., 2006b. Satellite-derived land surface parameters for mesoscale modeling of the Mexico City basin, Atmos. Chem. Phys., 6, 1315–1330.

Dentener F.J., Carmichael G.R., Zhang Y., Lelieveld J., and Crutzen P.J., 1996. Role of mineral aerosol as a reactive surface in the global troposphere. Journal Geophysical Research 101, 22869 – 22889.

Draxler R.R., Gillette D.A., Kirkpatrick J.S., Heller J., 2001. Estimating PM_{10} air concentrations from dust storms in Iraq, Kuwait and Saudi Arabia. Atmospheric Environment 35, 4315-4330.

Dzepina, K., J. Arey, L.C. Marr, et al. Detection of Particle-Phase Polycyclic Aromatic Hydrocarbons in Mexico City using an Aerosol Mass Spectrometer. International Journal of Mass Spectrometry, 263(2-3), 152-170, 2007.

Dzepina, K., R.M. Volkamer, S. Madronich, P. Tulet, I.M. Ulbrich, Q. Zhang, C.D. Cappa, P.J. Ziemann, and J.L. Jimenez. Evaluation of New Secondary Organic Aerosol Models for a Case Study in Mexico City. Atmospheric Chemistry and Physics, in press, 2009.

Environ, 2003. User's guide to the comprehensive air quality model with extensions (CAMx), version 4.02, report, ENVIRON Int. Corp., Novato, Calif., Available at http://www.camx.com.

Fahey K. and Pandis S.N., 2001 Optimizing model performance: variable size resolution in cloud chemistry modeling, Atmospheric Environment 35, 4471-4478.

Feingold G., Cotton W.R., Kreidenweis S.M., and Davis J.T., 1999. The impact of giant cloud condensation nuclei on drizzle formation in stratocumulus: Implications for cloud radiative properties. Journal of the Atmospheric Sciences 56, 4100– 4117.

Finlayson-Pitts B.J. and Pitts J.N., 2000. Chemistry of the Upper and Lower Atmosphere, Academic Press, San Diego, pp 281-286.

Fountoukis C. and Nenes A.: ISORROPIA-II: a computationally efficient thermodynamic equilibrium model for K^+-Ca^{2+}-Mg^{2+}-NH_4^+-Na^+-SO_4^{2-} -NO_3^- -Cl^- -H_2O aerosols. Atmospheric Chemistry and Physics 7, 4639-4659, 2007.

Fountoukis C., Nenes A., Sullivan A., Weber R., VanReken T., Fischer M., Matias E., Moya M. Farmer D., and Cohen R., 2009. Thermodynamic characterization of Mexico City Aerosol during MILAGRO 2006. Atmospheric Chemistry and Physics 9, 2141-2156.

Gaydos T., Koo B., and Pandis S.N., 2003. Development and application of an efficient moving sectional approach for the solution of the atmospheric aerosol condensation/evaporation equations. Atmospheric Environment 37, 3303-3316.

Gaydos T., Pinder R., Koo B., Fahey K., Yarwood G. and Pandis S.N., 2007. Development and application of a three-dimensional Chemical Transport Model, PMCAMx. Atmospheric Environment 41, 2594–2611.

Gillies J.A., Gertler A.W., Sagebiel J.C., and Dippel W.A., 2001. On-road particulate matter ($PM_{2.5}$ and PM_{10}) emissions in the Sepulveda Tunnel, Los Angeles, California. Environmental Science and Technology 35, 1054-1063.

Grell G.A., Dudhia J., and Stauffer D.R., 1995. A description of the Fifth-Generation Penn State/NCAR Mesoscale Model (MM5), NCAR/TN-398+STR, Natl. Cent. for Atmos. Res., Boulder, Colo, Available at http://www.mmm.ucar.edu/mm5/documents/mm5-desc-doc.html.

Gutierrez-Castorena M.D., Stoops G., Solorio C.A.O., Avila G.L., 2005.Amorphous silica materials in soils and sediments of the Ex-Lago de Texcoco, Mexico: An explanation for its subsidence. CATENA 80, 205-226.

Hennigan, C. J., Sullivan, A. P., Fountoukis, C. I., Nenes, A., Hecobian, A., Vargas, O., Peltier, R. E., Case Hanks, A. T., Huey, L. G., Lefer, B. L., Russell, A. G., and Weber, R. J.: On the volatility and production mechanisms of newly formed nitrate and water soluble organic aerosol in Mexico City, Atmos. Chem. Phys., 8, 3761-3768, 2008.

Jacob D.J., 2000. Heterogeneous chemistry and tropospheric ozone. Atmospheric Environment 34, 2131– 2159.

Jacobson M.Z., Tabazadeh A., and Turco R.P., 1996. Simulating equilibrium within aerosols and nonequlibrium between gases and aerosols. Journal of Geophysical Research 101, 9079–9091.

Jacobson M.Z., 1997a. Development and application of a new air pollution modeling system - II: Aerosol module structure and design. Atmospheric Environment 31A, 131-144.

Jacobson M.Z., 1997b. Numerical techniques to solve condensational and dissolutional growth equations when growth is coupled to reversible reactions. Aerosol Science Technology 27, 491-498.

Jacobson M.Z., 1999a. Chemical Equilibrium and Dissolution Processes, Fundamentals of Atmospheric Modeling, Cambridge University Press, New York, 476–510.

Jacobson M.Z., 1999b. Studying the effect of calcium and magnesium on size-distributed nitrate and ammonium with EQUISOLV II. Atmospheric Environment 33, 3635–3649.

Jayne J.T., Leard D.C., Zhang X., Davidovits P., Smith K.A., Kolb C.E., and Worsnop D.R., 2000. Development of an Aerosol Mass Spectrometer for size and composition analysis of submicron particles. Aerosol Science and Technology 33, 49–70.

Jimenez J.L., Jayne J.T., Shi Q., Kolb C.E., Worsnop D.R., Yourshaw I., Seinfeld J.H., Flagan R.C., Zhang X., Smith K.A., Morris J., and Davidovits P., 2003. Ambient aerosol sampling using the Aerodyne Aerosol Mass Spectrometer. Journal of Geophysical Research 108, 8425, doi:10.1029/2001JD001213.

Johnson K.S., de Foy B., Zuberi B., Molina L.T., Molina M.J., Xie Y., Laskin A., and Shutthanandan V., 2006. Aerosol composition and source apportionment in the Mexico City Metropolitan Area with PIXE/PESA/STIM and multivariate analysis. Atmospheric Chemistry and Physics 6, 4591–4600.

Johnson K.S., Laskin A., Jimenez J.L., Shutthanandan V., Molina L.T., Salcedo D., Dzepina K., and Molina M.J., 2008. Comparative analysis of urban atmospheric aerosol by Particle-Induced X-ray Emission (PIXE), Proton Elastic Scattering Analysis (PESA), and Aerosol Mass Spectrometry (AMS). Environmental Science and Technology 42, 6619-6624.

Karydis V.A., Tsimpidi A.P., Pandis S.N., 2007. Evaluation of a three-dimensional chemical transport model (PMCAMx) in the eastern United States for all four seasons. Journal of Geophysical Research 112, doi:10.1029/2006JD007890.

Kim Y.P., Seinfeld J.H., and Saxena P., 1993a. Atmospheric gas – aerosol equilibrium I. Thermodynamic model. Aerosol Science and Technology 19, 157–181.

Kim Y.P., Seinfeld J.H., and Saxena P., 1993b. Atmospheric gas – aerosol equilibrium II. Analysis of common approximations and activity coefficient calculation methods. Aerosol Science Technology 19, 182–198.

Kim Y.P. and Seinfeld J.H., 1995. Atmospheric gas – aerosol equilibrium III. Thermodynamics of crustal elements Ca^{2+}, K^{+}, and Mg^{2+}. Aerosol Science and Technology 22, 93–110.

Kleinman, L. I., Springston, S. R., Daum, P. H., Lee, Y.-N., Nunnermacker, L. J., Senum, G. I., Wang, J., Weinstein-Lloyd, J., Alexander, M. L., Hubbe, J., Ortega, J., Canagaratna, M. R., and Jayne, J.: The time evolution of aerosol composition over the Mexico City plateau, Atmos. Chem. Phys., 8, 1559-1575, 2008.

Koo B., Pandis S.N., and Ansari A., 2003. Integrated approaches to modeling the organic and inorganic atmospheric aerosol components. Atmospheric Environment 37, 4757-4768.

Kumar P., Sokolik I.N., and Nenes A., 2009. Parameterization of cloud droplet formation for global and regional models: including adsorption activation from insoluble CCN. Atmospheric Chemistry and Physics 9, 2517-2532.

Lane T.E., Donahue N.M., and Pandis S.N., 2008. Simulating secondary organic aerosol formation using the volatility basis-set approach in a chemical transport model. Atmospheric Environment 42, 7439-7451.

Lei, W., de Foy, B., Zavala, M., Volkamer, R., and Molina, L. T, 2007. Characterizing ozone production in the Mexico City Metropolitan Area: a case study using a chemical transport model, Atmos. Chem. Phys., 7, 1347-1366.

Lei, W., Zavala, M., de Foy, B., Volkamer, R., Molina, M. J., and Molina, L. T., 2009. Impact of primary formaldehyde on air pollution in the Mexico City Metropolitan, Atmos. Chem. Phys., 9, 2607-2618.

Li J., Zhuang G.S., Huang K., Lin Y.F., Xu C., and Yu S.L., 2008. Characteristics and sources of air-borne particulate in Urumqi, China, the upstream area of Asia dust. Atmospheric Environment 42, 776-787.

Liao H., Adams P.J., Chung S.H., Seinfeld J.H., Mickley L.J., and Jacob D.J., 2003. Interactions between tropospheric chemistry and aerosols in a unified general circulation model. Journal of Geophysical Research 108, 4001, doi:10.1029/2001JD001260.

Lurmann F.W., Wexler A.S., Pandis S.N., Musarra S., Kumar N., Seinfeld J.H., 1997. Modeling urban and regional aerosols - II. Application to California's south coast air basin. Atmospheric Environment 31, 2695-2715.

Mahowald N.M., and Kiehl L.M., 2003. Mineral aerosol and cloud interactions. Geophysical Research. Letters 30, 1475, doi:10.1029/2002GL016762.

Marcazzan G.M., Vaccaro S., Valli G., and Vecchi R., 1997. Characterisation of chemical species in PM2.5 and PM10 aerosols in Brisbane, Australia. Atmospheric Environment 31, 3773-3785.

Martin R.V., Jacob D.J., Yantosca R.M., Chin M., and Ginoux P., 2003. Global and regional decreases in tropospheric oxidants from photochemical effects of aerosols. Journal of Geophysical Research 108, 4097, doi:10.1029/2002JD002622.

McKendry I.G., Hacker J.P., Stull R., Sakiyama S., Mignacca D., and Reid K., 2001. Long-range transport of Asian dust to the lower Fraser Valley, British Columbia, Canada. Journal of Geophysical Research 106, 18361–18370.

Mebust M.R., Eder B.K., Binkowski F.S., and Roselle S.J., 2003. Models-3 Community Multiscale Air Quality (CMAQ) model aerosol component: 2. Model evaluation. Journal Geophysical Research 108, 4184, doi:10.1029/2001JD001410.

Meng Z., Seinfeld J.H., 1996. Time scales to achieve atmospheric gas-aerosol equilibrium for volatile species. Atmospheric Environment 30, 2889-2900.

Meng Z.Y., Seinfeld J.H., Saxena P., and Kim Y.P., 1995. Atmospheric gas – aerosol equilibrium IV. Thermodynamics of carbonates. Aerosol Science and Technolpgy 23, 131–154.

Meng Z., Dabdub D., Seinfeld J.H., 1998. Size-resolved and chemically resolved model of atmospheric aerosol dynamics. Journal of Geophysical Research 103, 3419-3435.

Moffet R.C., de Foy B., Molina L.T., Molina M.J. and Prather K.A., 2008. Measurement of ambient aerosols in northern Mexico City by single particle mass spectrometry. Atmospheric Chemistry and Physics 8, 4499-4516.

Molina L.T., Kolb CE, de Foy B., Lamb B.K., Brune W.H., Jimenez J.L., Ramos-Villegas R., Sarmiento J., Paramo-Figueroa V.H., Cardenas B., Gutierrez-Avedoy V., and Molina M.J. 2007. Air quality in North America's most populous city - overview of the MCMA-2003 campaign, Atmos. Chem. Phys., 7, 2447– 2473.

Molina L.T., Madronich S., Gaffney J.S., and Singh H.B., 2008. Overview of MILAGRO/INTEX-B Campaign, IGAC Newsletter, 38, 2-15.

Morris R.E., Koo B., Guenther A., Yarwood G., McNally D., Tesche T.W., Tonnesen G., Boylan J., and Brewer P., 2006. Model sensitivity evaluation for organic carbon using two multi-pollutant air quality models that simulate regional haze in the southeastern United States, Atmospheric Environment 40, 4960–4972.

Moya M., Pandis S.N., and Jacobson M.J., 2002. Is the size distribution of urban aerosols determined by thermodynamic equilibrium? An application to Southern California. Atmospheric Environment 36, 2349–2365.

Moya M., Ansari A.S., and Pandis S.N., 2001. Partitioning of nitrate and ammonium between the gas and particulate phases during the 1997 IMADA-AVER study in Mexico City. Atmospheric Environment 35, 1791–1804.

Nenes A., Pandis S.N., and Pilinis, C., 1998. ISORROPIA: A new thermodynamic equilibrium model for multiphase multicomponent inorganic aerosols. Aquatic Geochemistry 4, 123–152.

Nenes A., Pilinis C., and Pandis S.N., 1999. Continued development and testing of a new thermodynamic aerosol module for urban and regional air quality models. Atmospheric Environment 33, 1553– 1560.

Nguyen M.T., Jamka A.J., Cazar R.A., and Tao F.M., 1997. Structure and stability of the nitric acid–ammonia complex in the gas phase and in water. Journal of Chemistry and Physics 106, 8710-8717.

Pandis S.N., Wexler A.S., Seinfeld J.H., 1993. Secondary organic aerosol formation and transport - II. Predicting the ambient secondary organic aerosol size distribution. Atmospheric Environment 27A, 2403-2416.

Park S.H., Song C.B., Kim M.C., Kwon S.B., and Lee K.W., 2004. Study on size distribution of total aerosol and water-soluble ions during an Asian dust storm event at Jeju Island, Korea. Environmental Monitoring and Assessment 93, 157-183.

Perry K.D., Cahill T.A., Eldred R.A., Dutcher D.D., and Gill T.E., 1997. Long-range transport of North African dust to the eastern United States. Journal Geophysical Research 102, 11225–11238.

Pilinis C., Seinfeld J.H., 1987. Continued development of a general equilibrium model for inorganic multicomponent atmospheric aerosols. Atmospheric Environment 21, 2453-2466.

Pilinis C., Capaldo K.P., Nenes A., Pandis S.N., 2000. MADM - A new multicomponent aerosol dynamics model. Aerosol Science Technology 32, 482-502.

Pitzer K.S. and Simonson J.M., 1986. Thermodynamics of multicomponent, miscible, ionic systems: Theory and equations. Journal of Physical Chemistry 90, 3005–3009.

Pope C.A., Burnett R.T., Thun M.J., Calle E E., Krewski D., Ito K., and Thurston G.D., 2002. Lung cancer, cardiopulmonary mortality, and long-term exposure to fine particulate air pollution. Journal of the American Medical Association 287, 1132–1141.

Prospero J.M., Ginoux P., Torres O., Nicholson S.E., and Gill T.E., 2002. Environmental characterization of global sources of atmospheric soil dust identified with the Nimbus 7 Total Ozone Mapping Spectrometer (TOMS) absorbing aerosol product. Reviews of Geophysics 40, 1002, doi:10.1029/2000RG000095.

Racherla P.N. and Adams P.J., 2006. Sensitivity of global tropospheric ozone and fine particulate matter concentrations to climate change. Journal of Geophysical Research-Atmospheres 111. doi:10.1029/2005JD006939.

Rudich Y., Khersonsky O., and Rosenfeld D., 2002. Treating clouds with a grain of salt. Geophysical Research Letters 29, 2060, doi:10.1029/2002GL016055.

Russell A.G., McCue K.F., Cass G.R., 1988. Mathematical modeling of the formation of nitrogen-containing air pollutants, 1. Evaluation of an Eulerian photochemical model. Environment Science Technology 22, 263-271.

Salcedo D., et al., 2006. Characterization of ambient aerosols in Mexico City during the MCMA-2003 campaign with aerosol mass spectrometry: Results at the CENICA supersite. Atmospheric Chemistry and Physics 6, 925–946.

San Martini F. M., West J. J., Sosa G., Molina L. T., Molina M. J., McRae G. J., 2005. Modeling inorganic aerosols and their response to changes in precursor concentration in Mexico City, *J. Air Waste Manage. Assoc*., 55 (6), 803–815, 2005.

San Martini, F.M., E.J. Dunlea, R. Volkamer, et al. Implementation of a Markov Chain Monte Carlo Method to Inorganic Aerosol Modeling of Observations from the MCMA-2003 Campaign. Part II: Model Application to the CENICA, Pedregal and Santa Ana Sites. Atmospheric Chemistry and Physics, 6, 4889-4904, 2006

Schwartz J., 1996. Air pollution and hospital admissions for respiratory disease. Epidermiology 7, 20–28.

Seinfeld J.H. and Pandis S.N., 2006. Atmospheric Chemistry and Physics: From Air Pollution to Climate Change, Hoboken, New Jersey, pp 381-383.

SMA-DF (Secretaria del Medio Ambiente del Distrito Federal), 2006. Inventario de Emisiones 2004 de la Zona Metropolitana del Valle de Mexico, Mexico.

Sun D., Lau K.M., and Kafatos M., 2008. Contrasting the 2007 and 2005 hurricane seasons: Evidence of possible impacts of Saharan dry air and dust on tropical cyclone activity in the Atlantic basin. Geophysical Research letters 35, doi:10.1029/2008GL034529.

Sun Q., Wexler A.S., 1998a. Modeling urban and regional aerosols near acid neutrality-application to the 24-25 June SCAQS episode. Atmospheric Environment 32, 3533-3545.

Sun Q., Wexler A.S., 1998b. Modeling urban and regional aerosols-condensation and evaporation near acid neutrality. Atmospheric Environment 32, 3527-3531.

Sposito G., 1989. The Chemistry of Soils, Oxford University Press.

Thomsen K. and Rasmussen P., 1999. Modeling of vapor-liquid-solid equilibrium in gas-aqueous electrolyte systems. Chemical Engineering Science 54, 1787–1802.

Tratt D.M., Frouin R.J., and Westphal D.L., 2001. April 1998 Asian dust event: A southern California perspective. Journal of Geophysical Research 106, 18371–18379.

Vega E., Mugica V. Reyes E., Sanchez G., Chow J.C., and Watson J.G., 2001. Chemical composition of fugitive dust emitters in Mexico City. Atmospheric Environment 35, 4033–4039.

Villasenor R., López-Villegas M.T. , Eidels-Dubovoi, S. ,Arturo Quintanar and Gallardo, J.C., 2003. A mesoscale modeling study of wind blown dust on the Mexico City Basin. Atmospheric Environment 37, 2451-2462.

Wang Y., Zhuang G.S., Tang A.H., Zhang W.J., Sun Y.L., Wang Z.F., and An Z.S., 2007. The evolution of chemical components of aerosols at five monitoring sites of China during dust storms. Atmospheric Environment 41, 1091-1106.

Wexler A.S. and Clegg S.L., 2002. Atmospheric aerosol models for systems including the ions H^+, NH_4^+, Na^+, SO_4^{2-}, NO_3^-, Cl^-, Br^-, and H_2O. Journal of Geophysical Research 107, 4207, doi:10.1029/2001JD000451.

Wurzler S., Reisin T.G., and Levin Z., 2000. Modification of mineral dust particles by cloud processing and subsequent effects on drop size distributions. Journal Geophysical Research 105, 4501– 4512.

Yu S., Dennis R., Roselle S., Nenes A., Walker J., Eder B., Schere K., Swall J., and Robarge W., 2005. An assessment of the ability of three-dimensional air quality models with current thermodynamic equilibrium models to predict aerosol NO_3^-. Journal of Geophysical Research 110, doi:10.1029/2004JD004718.

Zaveri R.A., Easter R.C., and Peters L.K., 2005a. A computationally efficient multicomponent equilibrium solver for aerosols (MESA). Journal of Geophysical Research 110, doi:10.1029/2004JD005618.

Zaveri R.A., Easter R.C., and Wexler A.S., 2005b. A new method for multicomponent activity coefficients of electrolytes in aqueous atmospheric aerosols. Journal of Geophysical Research 110, doi:10.1029/2004JD004681.

Zaveri R.A., Easter R.C., Fast J.D., Peters L.K., 2008. Model for Simulating Aerosol Interactions and Chemistry (MOSAIC). Journal of Geophysical Research-Atmospheres 113, doi: 10.1029/2007JD008782.

Zhang K.M. and Wexler A.S., 2008. Modeling urban and regional aerosols - Development of the UCD Aerosol Module and implementation in CMAQ model. Atmospheric Environment 42, 3166-3178.J. Zheng, R. Zhang, E.C. Fortner, et al. Measurements of HNO_3 and N_2O_5 Using Ion Drift - Chemical Ionization Mass Spectrometry during the MILAGRO/MCMA -2006 Campaign. Atmospheric Chemistry and Physics, 8, 6823-6838, 2008.

Table 1. Inorganic aerosol concentrations ($\mu g\ m^{-3}$) at the boundaries of the domain

Species	South Boundary	West Boundary	East Boundary	North Boundary
Sulfate	1.2	3	0.9	2.3
Ammonium	0.15	1	0.2	0.7
Nitrate	0.8	0.25	0.6	0.6
Chloride	2.8	0.8	1	1.2
Sodium	2.5	0.7	1	1.2

Table 2. Description of Mexico City Sites

Site and position	**Site description**
CENICA (N19.358^o, W99.073^o)	MCMA-2003 super site located in the Autonomous Metropolitan University campus Iztapalapa at the southeast of the city.
Constituyentes (N19.400^o, W99.210^o)	Western suburban neighborhood close to Chapultepec park.
La Merced (N19.424^o, W99.119^o)	Central city section.
La Reforma (N19.976^o, W98.697^o)	Southwestern downwind site from Pachuca, city with 245 000 inhabitants located to the northeast of Mexico City.
Pedregal (N19.325^o, W99.204^o)	Southwestern suburban neighborhood.
Santa Ana Tlacotenco (N19.177^o, W98.990^o)	Rural site to the southwest of Mexico City, close to the gap in the mountains at Amecameca.
Teotihucan (N19.688^o, W98.870^o)	Northern upwind boundary site of Mexico City.
Xalostoc (N19.527^o, W99.076^o)	North-eastern industrial section of the city with light to medium industries.
T0 (N19.489^o, W99.148^o)	Urban background site located to the northwestern part of the basin of Mexico City.
T1 (N19.703^o, W98.982^o)	Suburban background site located around 50 km to the north of Mexico City, in an area isolated from major urban agglomerations but close to small populated agglomerations.
T2 (N20.010^o, W98.909^o)	Regional background site located around 90 km to the north of the city of Mexico, in the surroundings of a farm isolated from major urban agglomerations.

Table 3. Comparison of PMCAMx predictions with hourly measurements taken at CENICA supersite during 13-16 of April 2003 (96 data points).

	Mean Observed ± Standard Deviation ($\mu g\ m^{-3}$)	Mean Predicted ± Standard Deviation ($\mu g\ m^{-3}$)	Mean Absolute Gross Error ($\mu g\ m^{-3}$)	Mean Bias ($\mu g\ m^{-3}$)	Normalized Mean Error (%)	Normalized Mean Bias (%)	Root Mean Square Error ($\mu g\ m^{-3}$)
PM_1 Sulfate	2.9±1	2.4±0.5	0.87	-0.57	30	-20	1.22
PM_1 Nitrate	3.1±3.5	3±4	2.31	-0.1	75	-3	3.35
PM_1 Ammonium	1.8±0.9	1.4±1.3	0.98	-0.36	56	-20	1.20
PM_1 Chloride	0.2±0.2	0.1±0.1	0.14	-0.06	78	-35	0.25

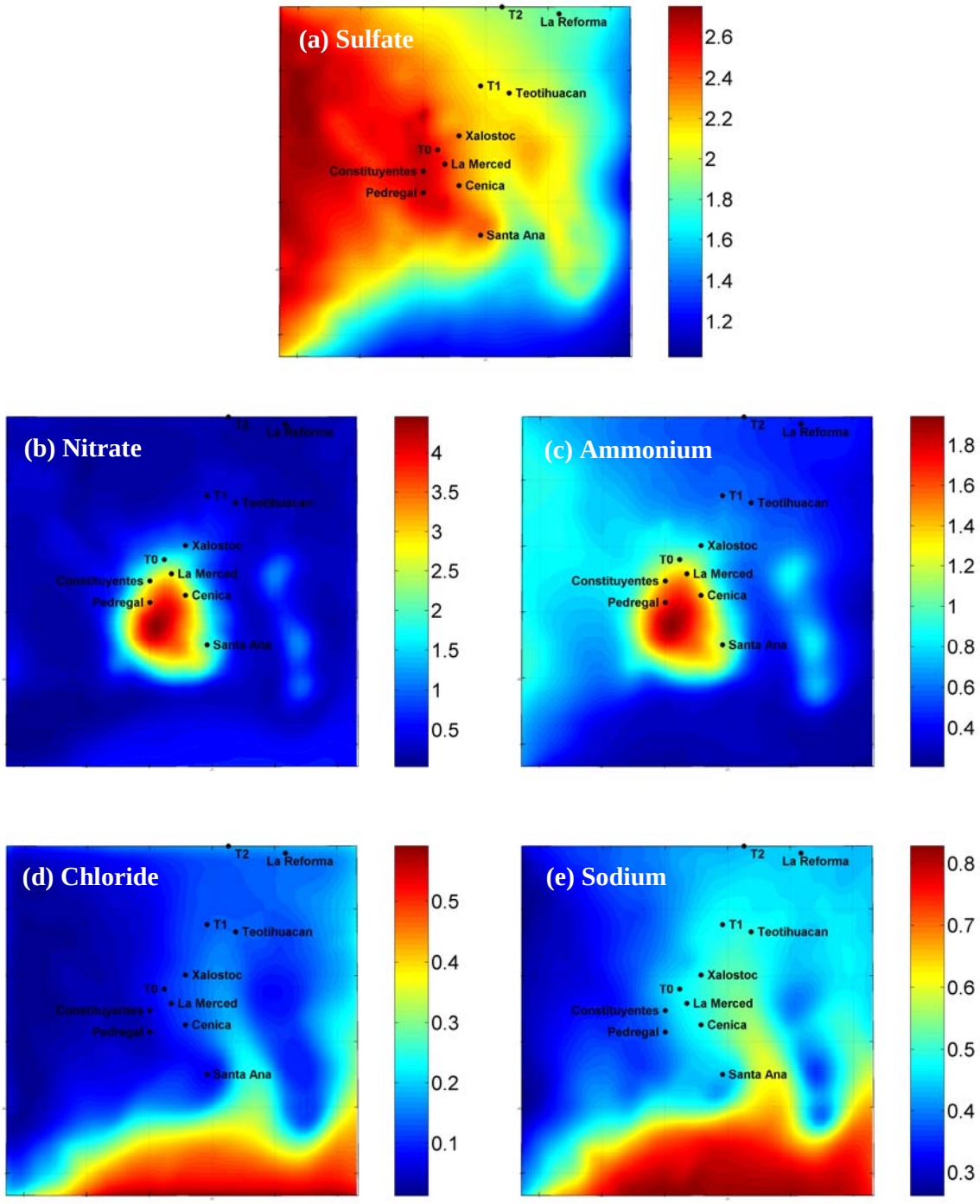

Figure 1. Predicted average ground level concentrations (μg m^{-3}) of PM_1 (fine) (a) sulfate, (b) nitrate, (c) ammonium, (d) chloride, and (e) sodium during 13-16 of April 2003.

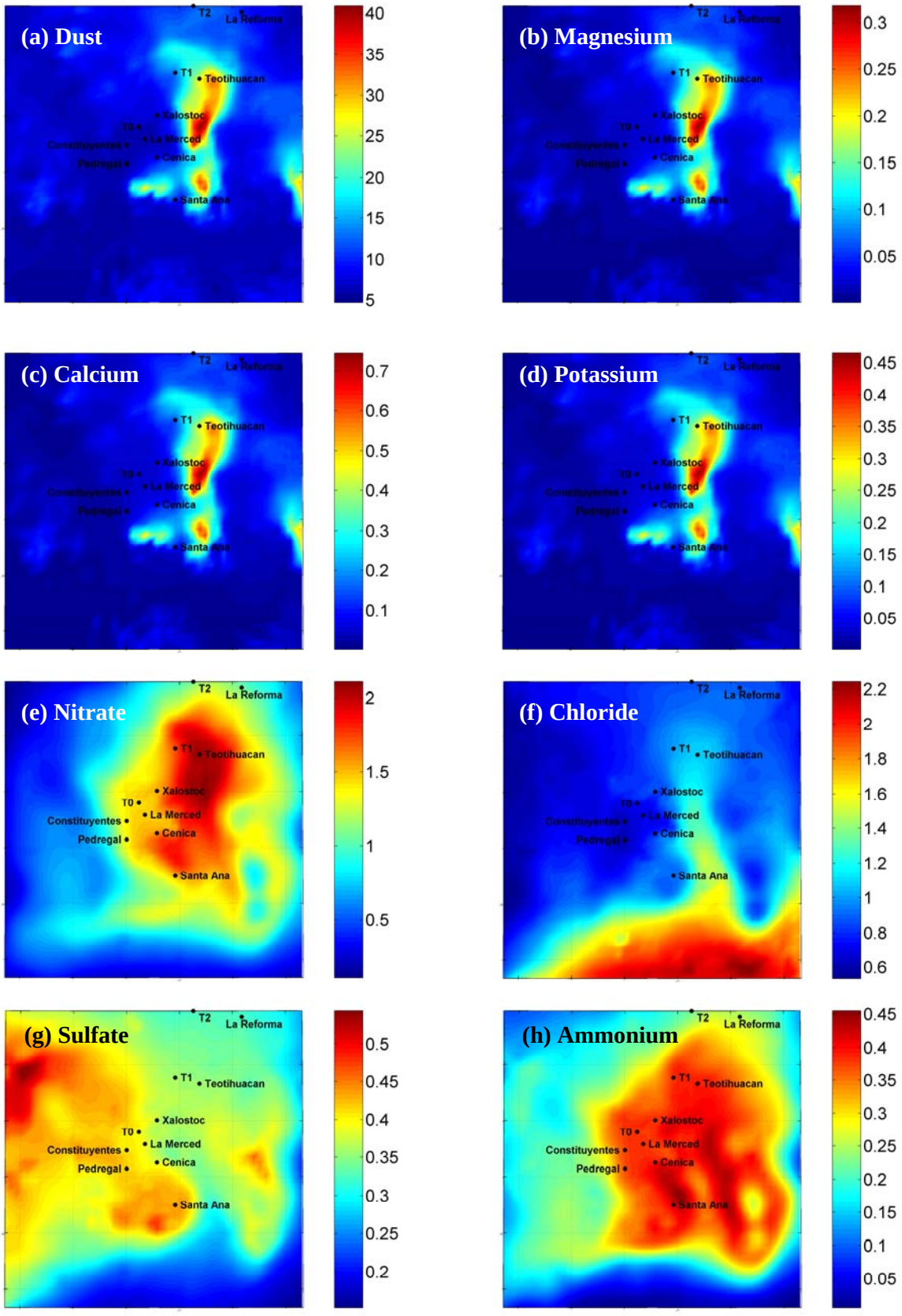

Figure 2. Predicted average ground level concentrations (μg m^{-3}) of $PM_{1\text{-}10}$ (coarse) (a) inert dust, (b) magnesium, (c) calcium, (d) potassium, (e) nitrate, (f) chloride, (g) sulfate and (h) ammonium during 13-16 of April 2003.

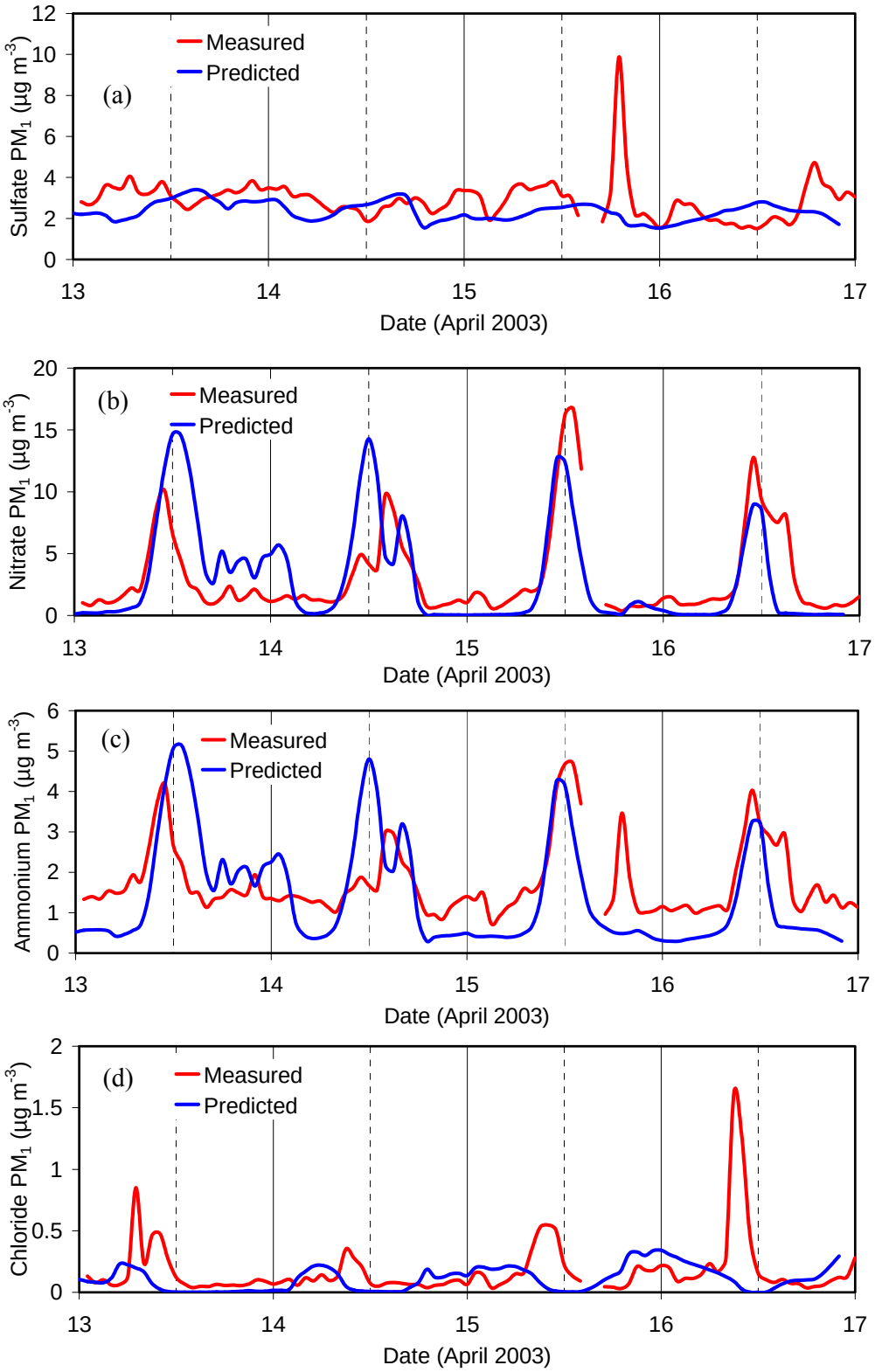

Figure 3. Comparison of model predictions with hourly average measurements taken at CENICA during the MCMA 2003 campaign for (a) PM_1-sulfate, (b) PM_1-nitrate, (c) PM_1-ammonium, and (d) PM_1-chloride

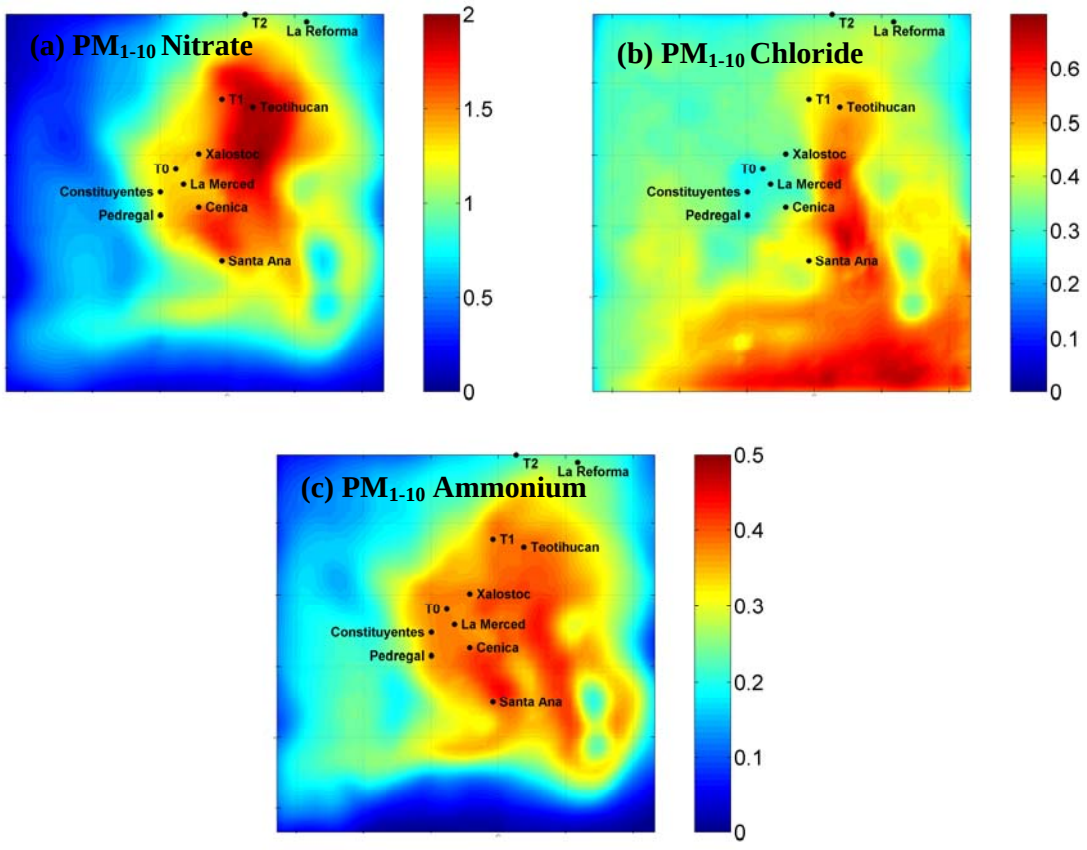

Figure 4. Predicted average ground level concentration increase (μg m^{-3}) from PMCAMx-2004 predictions for (a) PM_{1-10} nitrate, (b) PM_{1-10} chloride, and (c) PM_{1-10} ammonium during 13-16 of April 2003. Increased concentrations are due to the explicit description of the crustal material thermodynamics and competition with the fine PM for semivolatile inorganic vapors.

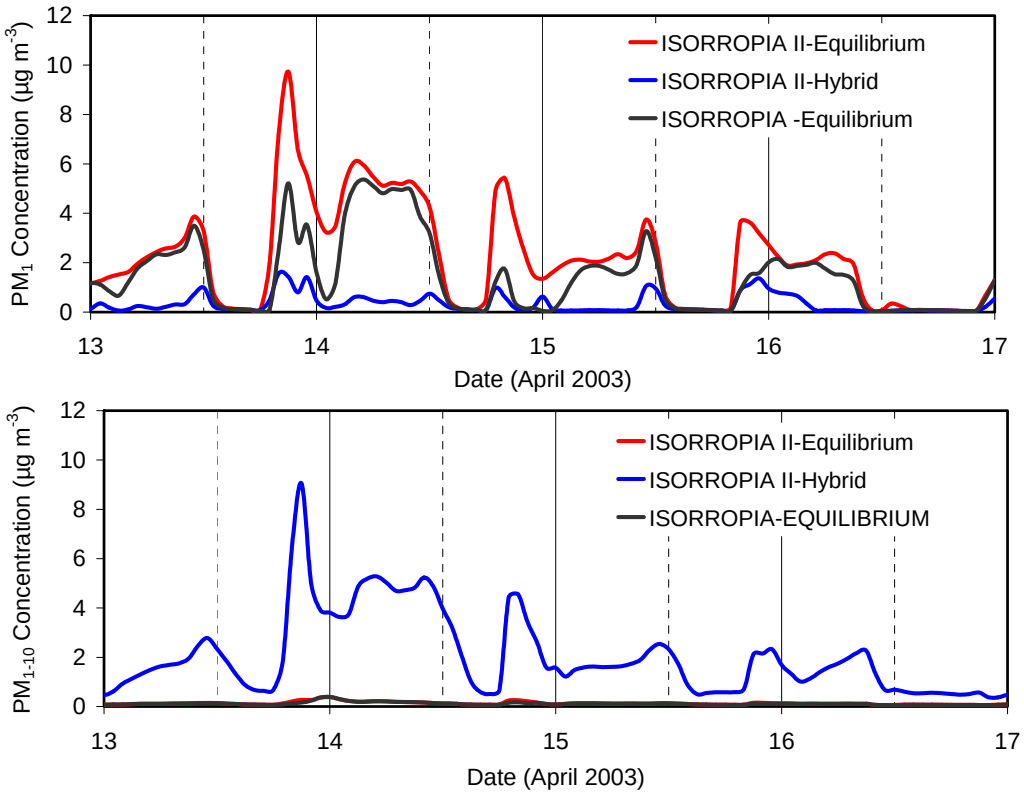

Figure 5. Comparison of model predictions using (i) ISORROPIA along with the equilibrium approach, (ii) ISORROPIA II along with the equilibrium approach, and (iii) ISORROPIA II along with the hybrid approach for PM_1 and $PM_{1\text{-}10}$ nitrate at Teotihuacan.

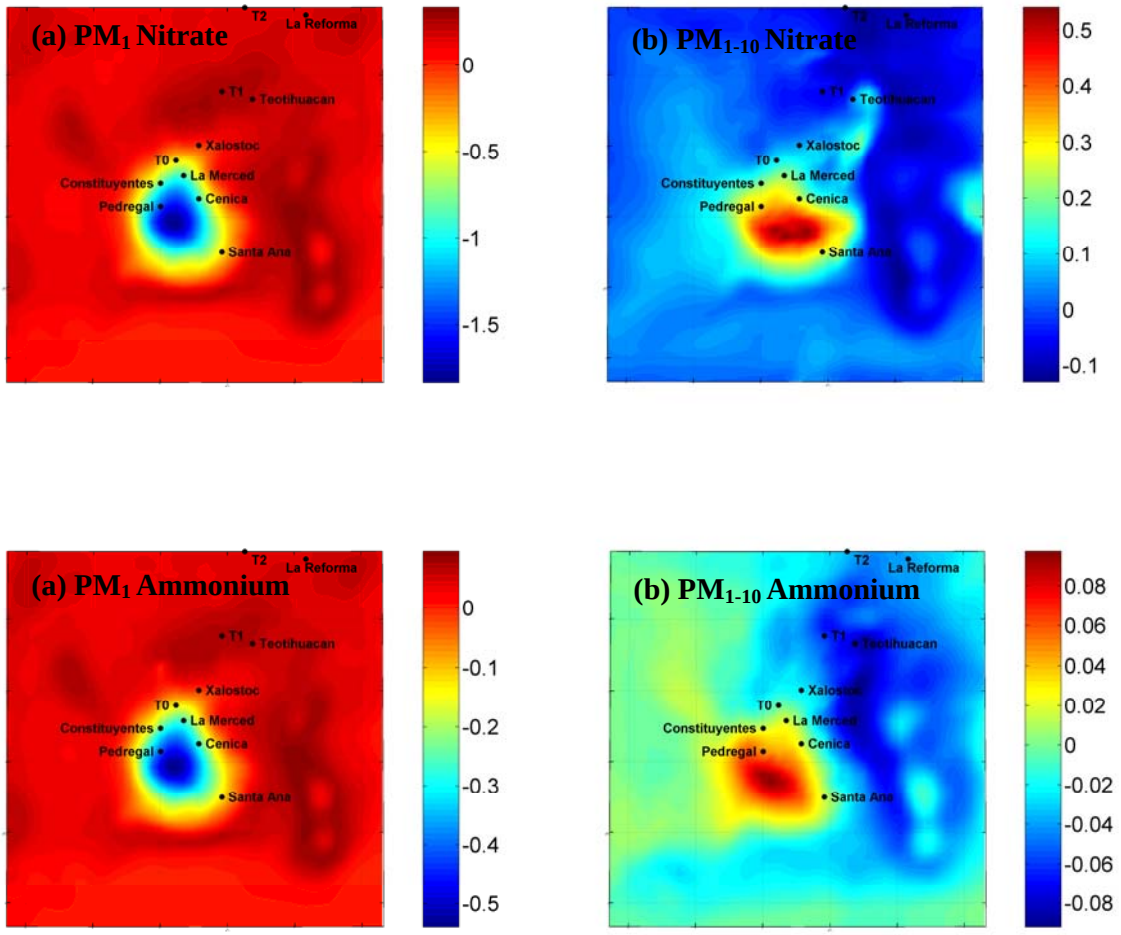

Figure 6. Predicted average ground level concentration change (Metastable – Stable) (μg m^{-3}) of (a) PM_1 nitrate, (b) PM_{1-10} nitrate, (c) PM_1 ammonium and (d) PM_{1-10} ammonium during 13-16 of April 2003 after assuming "metastable" aerosols. A negative change corresponds to lower concentrations in the metastable case.

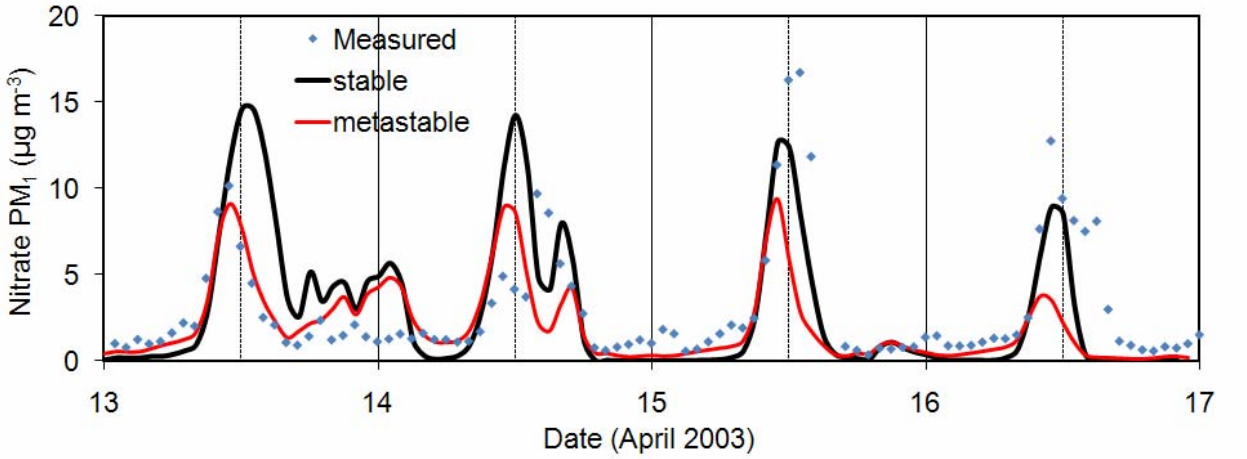

Figure 7. Comparison of model predictions, assuming stable and metastable aerosols, with hourly average measurements taken at CENICA during the MCMA 2003 campaign for PM_1-nitrate.